

# Design and Evaluation of a 32 Channel Phased Array Coil for Human Lung Imaging Using Hyperpolarized $^3\text{He}$

F. M. Meise<sup>1</sup>, J. Rivoire<sup>1</sup>, G. C. Wiggins<sup>2,3</sup>, B. Keil<sup>4</sup>, M. Terekhov<sup>1</sup>, D. Santoro<sup>1</sup>, Z. Salhi<sup>5</sup>, S. Karpuk<sup>5</sup>, L. L. Wald<sup>2,3</sup>, and W. G. Schreiber<sup>1</sup>

<sup>1</sup>Section of Medical Physics, Department of Diagnostical and Interventional Radiology, Johannes Gutenberg University Medical School, Mainz, RLP, Germany, <sup>2</sup>Athinoula A. Martinos Center for Biomedical Imaging, Department of Radiology, MGH, Harvard Medical School, Charlestown, MA, United States, <sup>3</sup>Harvard-MIT Division of Health Sciences and Technology, <sup>4</sup>Department of Diagnostic Radiology, University Hospital, Philipps University, Marburg, Germany, <sup>5</sup>Institute of Physics, Johannes Gutenberg University, Mainz, Germany

## Introduction

In the last years imaging of the lungs with hyperpolarized  $^3\text{He}$  allowed analyses of the regional intrapulmonary  $\text{pO}_2$  or the microstructure of the lung (1). The high potential of these techniques is tempered by the long breath-holds (up to 40sec) necessary to acquire the needed functional data. In addition to patient discomfort, every RF-pulse diminishes the hyperpolarisation of the  $^3\text{He}$ . Because of these reasons, realising parallel imaging acceleration in  $^3\text{He}$  images is a main interest in today's lung imaging research (2). To understand and analyse the possibilities of parallel imaging of the lung, a 32-channel phased array was developed and compared with a standard single channel volume coil.

## Methods

The  $^3\text{He}$  array was designed for a 1.5T Avanto TIM (Siemens Medical Solutions, Erlangen, Germany) MRI system. To realise positioning of the receive elements close to the body a fibreglass shell (3) was build with 16 loop elements mounted on the top and 16 loop elements on the backside.. Because of cables running in the patient table the bottom part of the coil had to be shielded to prevent coupling to the transmit and receive elements. **Transmit coil:** For excitation, a transmit coil consisting of two square elements was designed with one mounted under the back and one above the chest Rx-elements. The Tx coil elements were feed by a Wilkinson divider and can be used as transmit/receive or transmit only. This facilitated measurement of B1-homogeneity and flip angle distribution. **Receive elements:** Rx-elements were tuned and matched with a slightly modified network as presented in (4). The elements can be actively detuned during the Tx-phase. RF fuses were placed in the element loop as a redundant safety backup in case the active detuning is broken.. To provide optimum decoupling between the elements, neighbored loops were decoupled by critical overlap and next nearest neighbours were decoupled by using active preamp decoupling (5). To prevent oscillations, the preamps were placed away from the Rx-elements and were connected to the coils via double shielded cables (G02232 cables, Huber Suhner, Essex Junction, VT, USA). A cable trap was implemented in front of the preamps to block common mode currents. **In Vivo imaging:** The coil went through an in-house-production process as described in the Medical Device Directive 93/42/EEC which includes a full risk assessment following the DIN ISO 14971 to assure patient safety. The phased array was tested with commonly used diagnostic protocols which were developed in the European PHIL-study for imaging morphology, diffusion and ventilation dynamics. Imaging was performed on the same subject once on conventional cardiovascular MRI system (Magnetom Sonata, Siemens Medical Solutions, Erlangen, Germany) with a double resonant ( $^3\text{He}/^{19}\text{F}$ ) birdcage coil (Rapid Biomedical, Rimpf, Germany) and on the Avanto TIM with the phased array coil. For imaging hyperpolarized gas with approx. 65 % polarization was used.

## Results

B1+ transmit inhomogenities were detected in both coils, likely due to residual coupling between  $^3\text{He}$  Tx coil and the scanner body coil. Nevertheless, an SNR increase up to a factor of 6 was observed compared to the  $^3\text{He}$  birdcage coil. High resolution 3D images were acquired with acceleration factors  $4 \times 2 = 8$  which still show very good SNR performance and almost no acceleration artefacts (Fig.4). With this scan time of the full lung was decreased by a factor of 6.

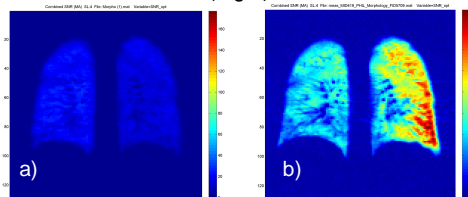


Fig2: Optimum SNR reconstructed SNR maps of a peripheral slice of the lung (a) Birdcage and (b) the 32channel array. In (b) 128 phase encoding steps had to be used instead of 81 in the single channel coil because of the SNR calculation script. Because of that the phased array SNR per voxel is 25% less than with the birdcage coil. Though a corrected maximum SNR gain by a factor of seven in the periphery can be observed.

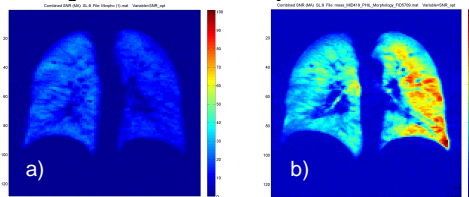


Fig.3: Optimum SNR reconstructed SNR map for comparison of a centre slice with (a) Birdcage and (b) the 32 channel array. Sequence parameters followed the PHIL protocol. Even in the centre an SNR gain up to a factor of five can be observed. The inhomogeneity in both images are probably caused by a coupling to the scanner's body coil

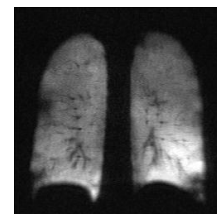


Fig.4: Slice from  $4 \times 2$  accelerated 3D imaging acquired in only 3sec. High detail of lung can be observed almost without any acceleration artefacts.

## Discussion

Prior to routine use, the coupling between the  $^3\text{He}$  coils and the scanner's body coil has to be analysed and mitigated. Nevertheless, the array shows a very good performance compared to the normally used single channel birdcage. The SNR gain up to a factor of seven can be either used to increase resolution, overcome the SNR degradation associated with highly accelerated imaging or utilize smaller doses of costly  $^3\text{He}$ . Finally patient comfort and compliance was improved by shortening the scan time by a factor of six.

## Reference

1. Schreiber WG et al. Respir Physiol Neurobiol 148 (2005) 23.
2. Lee RF et al. Magn Reson Med 2006;55(5):1132-1141.
3. Schmitt M et al. Magn Reson Med 2008;59(6):1431-1439.
4. Wiggins GC et al. Magn Reson Med 2006;56(1):216-223.
5. Roemer PB, et al. Magn Reson Med 1990;16(2):192-225.

## Acknowledgement

This work was supported by DFG SCHR 687/2; FOR 474 and the German Academic Exchange Service. Thanks to Bernd Stoeckel and Andreas Potthast from Siemens Medical Solutions.